Ultrafast transport and relaxation of hot plasmonic electrons in metal-dielectric heterostructures

Ilya Razdolski*
Fritz Haber Institute of the Max Planck Society, 14195 Berlin, Germany

Alexander L. Chekhov†
Department of Physics, Moscow State University, 119991 Moscow, Russia

Alexander I. Stognij
Scientific-Practical Materials Research Center of the NASB, 220072 Minsk, Belarus

Andrzej Stupakiewicz
Faculty of Physics, University of Bialystok, 15-245 Bialystok, Poland

(Received 28 January 2019; revised manuscript received 29 April 2019; published 16 July 2019)

Owing to the ultrashort timescales of ballistic electron transport, relaxation dynamics of hot nonequilibrium electrons is conventionally considered local. Utilizing propagating surface plasmon-polaritons (SPs) in metal-dielectric heterostructures, we demonstrate that both local (relaxation) and nonlocal (transport) hot electron dynamics contribute to the transient optical response. The data obtained in two distinct series of pump-probe experiments demonstrate a strong increase in both nonthermal electron generation efficiency and nonlocal relaxation timescales at the SP resonance. We develop a simple kinetic model incorporating a SP excitation, where both local and nonlocal electron relaxation in metals are included, and analyze nonequilibrium electron dynamics in its entirety in the case of collective electronic excitations. Our results elucidate the role of SPs in nonequilibrium electron dynamics and demonstrate rich perspectives of ultrafast plasmonics for tailoring spatiotemporal distribution of hot electrons in metallic nanostructures.

DOI: 10.1103/PhysRevB.100.045412

I. INTRODUCTION

Recent advances in femtosecond light-matter interaction have stimulated sheer fundamental interest to nonthermal electrons, envisioning a number of applications [1–7]. It is now widely accepted that the electron dynamics after an ultrashort optical excitation cannot be accurately described within the thermal equilibrium models. Instead, nonequilibrium electron distributions should be considered on the subpicosecond timescale [8–14]. The generation of hot, non-thermal electrons is strongly facilitated in plasmonic nanostructures, where elaborated relaxation models have been invoked to describe the experimental data [15]. Nonlocal relaxation of the nonthermal population through electron transport is often neglected, due to its sheer complexity and ultrashort timescales. Owing to the difficulties in applying purely ballistic or diffusive models, more complicated theoretical approaches were suggested [16]. Other works discuss electron dynamics in metal nanoparticles [17–22], thus minimizing the electron transport contributions, or deem ballistic electron transport too fast to be analyzed on equal footing with the local dynamics [23].

It can be argued, however, that for future photonic applications featuring surface plasmon (SP) excitation as building blocks, the transport of hot electrons is of prime importance. A few examples of relevant physical effects are the heat [24] and spin transport [25,26], as well as laser-induced magnetization dynamics [27–33]. As such, a comprehensive analysis of the ultrafast optical probing of spatial distribution of hot electrons in plasmonic nanostructures remains a highly desirable perspective.

Of particular interest is the electron transport contribution to the optical response of a remote metallic interface, where the impact of the optical pump is negligible. In this paper, we experimentally realize this approach in a pump-probe scheme and develop a simple kinetic model for both local and nonlocal relaxation of hot electrons. Our results show that SPs can be utilized for engineering the spatiotemporal properties of the hot electron population. Continuously varying the pump wavelength across the SP resonance, we observe significant increase of the hot electron transport timescale in the time-resolved transmittance and attribute it to the SP excitation. Further, we show how the relaxation dynamics of hot electrons can give information about the surface plasmon lifetimes at arbitrary interfaces. Showing a high degree of consistency in the determination of the SP and hot electron lifetimes, our results elucidate the previously unexplored role of SP excitation in the nonequilibrium electron dynamics.

*Present address: FELIX laboratory, Radboud University, 6525 HP Nijmegen, The Netherlands; ilyar@science.ru.nl
†Present address: Department of Physics, Free University Berlin, 14195 Berlin, Germany.

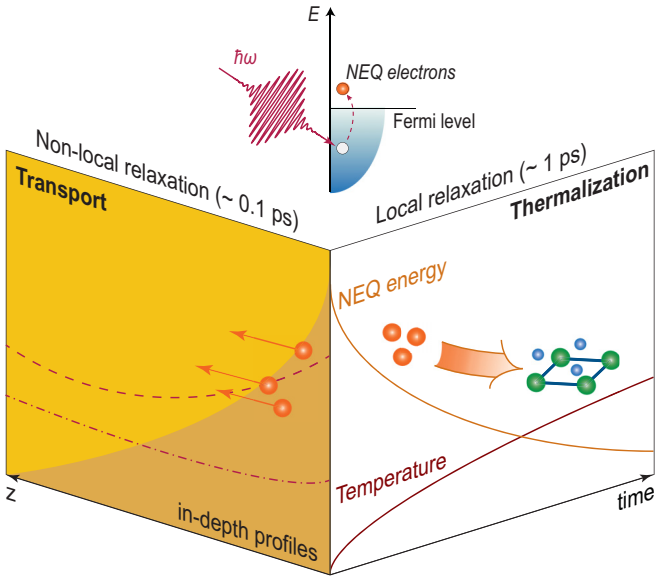

FIG. 1. The electron dynamics upon ultrafast laser excitation of a thick metal film. Left: Nonthermal population (the shaded area) is created within the optical penetration depth ζ. Transport of hot electrons leads to the in-depth redistribution (dashed and dash-dotted lines) and nonlocal relaxation of their population. Right: Thermalization of hot electrons (local relaxation) results in the temperature rise. The inset illustrates energy flow from the nonequilibrium electrons (orange) to the thermalized electrons (blue) and lattice (green). The top inset shows the laser-induced creation of the nonthermal electrons population.

II. THEORY

Femtosecond laser excitation of metals results in the generation of hot electrons above the Fermi level (Fig. 1, inset). The spatial distribution of these primary electrons is governed by the optical excitation profile, typically [for plasmonic metals (PM) in the near-infrared spectral range] on the order of 20 nm. As such, in thicker PM films, the excitation inhomogeneity enables subsequent in-depth redistribution of the hot electron population (Fig. 1, left). Superdiffusive and ballistic transport mechanisms have been argued to play a key role on the ultrafast timescale [28,34,35]. In Au, large mean free path values ($\gtrsim$100 nm) for hot electrons [25,34,36,37] indicate the ballistic character of the electron transport with the Fermi velocity $v_F \sim 1$ nm/fs.

The laser-generated nonequilibrium population of hot electrons decays through electron-electron and electron-phonon scattering (Fig. 1, right). Experimentally, the importance of nonequilibrium electron distribution for the ultrafast transient optical response has been established in various metals [11,12,23,38]. The lifetime of the nonequilibrium electron distribution τ_N was found to be $\sim 0.5-1$ ps. We emphasize that this τ_N should not be confused with the average single electron lifetime $\tau_e \sim 10-30$ fs at electron energies $E \sim 1$ eV, as predicted by the Fermi liquid theory and measured in photoemission experiments [39–41]. This striking difference is related to the electron multiplication, resulting in the temporary increase of the number of nonthermal electrons and the lifetime of their population. Until the electron distribution is relaxed to the Fermi-Dirac one, the two-temperature model description utilizing well-defined electron and lattice temperatures cannot be employed. Eventually, the electron-phonon system relaxes towards thermal equilibrium at an elevated temperature (Fig. 1). All these processes contribute to the transient properties of PM systems and can be identified from the time-resolved optical experiments.

Analyzing the typical timescales, it becomes clear that in $\lesssim$100-nm-thick PM films, ballistic transport of hot laser-excited electrons occurs on a much faster timescale than the electron thermalization. Thus, although both electron transport and thermalization contribute to the transient variations of the optical properties in an intricate way, the disparity of the timescales enables the experimental disentanglement of these effects. Spitzer *et al.* [42] reported $\tau_{S1} \approx 220-300$ fs, $\tau_{S2} \approx 940$ fs in a 130-nm-thick Au layer, claiming the relaxation of the hot electrons within $30-80$ fs and therefore excluding it from consideration. However, previous studies of hot electrons in PMs [10–12,23] suggest much longer relaxation times of the nonthermal electronic population (up to 1 ps). This underestimation of the effective lifetime of hot electrons and its lack of sensitivity to the excitation of SP resonance prompted the authors to look for alternative explanations.

III. EXPERIMENTAL RESULTS

To reveal the role of the SP excitation in the ultrafast hot electron dynamics, in this paper we employed 40-fs-long laser pulses for studying transient transmittance of a periodically corrugated Au/Co-doped yittrium iron garnet (YIG:Co) magnetoplasmonic crystal. This ferrimagnetic dielectric garnet is a promising material for magnetic recording applications [43] whereas photonic excitations can be utilized for the nanoscale localization of the laser-excited spin dynamics [44–46]. The metallic grating enables free-space excitation of propagative SPs [42,46–53], according to the well-known phase-matching condition $k_{SP} = k_0 \sin\theta + mk_G$. Here k_{SP} is the SP wave vector, $k_{in} = k_0 \sin\theta$ is the in-plane component of the free-space photon momentum, $k_G = 2\pi/b$ is the quasi-wave-vector of a grating of period b, and m is an integer. Transmittance angular spectra of the magnetoplasmonic Au-YIG:Co crystal with $b =$ 800 nm, gap width 100 nm, and Au thickness $d = 50$ nm [46] at a series of fundamental wavelengths [Fig. 2(a)] illustrate the SP dispersion in the near-IR range. In the first series of time-resolved measurements, the pump (fluence $\sim$1 mJ/cm^2) angle of incidence was fixed at $\theta_p = 24^\circ$, and its wavelength λ_p was tuned around the SP resonance at the Au/garnet interface at about $\lambda_{SP} \approx 1.3$ μm, close to the resonance in the laser-induced magnetization switching in YIG:Co [43]. The typical time-resolved trace of the transmittance variations $\Delta T(t)$ of the delayed, weak probe beam at 800-nm wavelength is shown in Fig. 2(b).

Taking into account the relevant physical processes at this timescale, we fitted the double exponential function to the set of transmittivity data obtained at various pump wavelengths:

$$\Delta T(t) \propto A_1 e^{-t/\tau_1} + A_2 e^{-t/\tau_2} + A_3(1 - e^{-t/\tau_2}). \quad (1)$$

This shape was convoluted with the Heaviside function $\Theta(t)$ with the finite step-width set to account for the duration of the cross-correlation pump-probe signal $w \approx 60$ fs measured

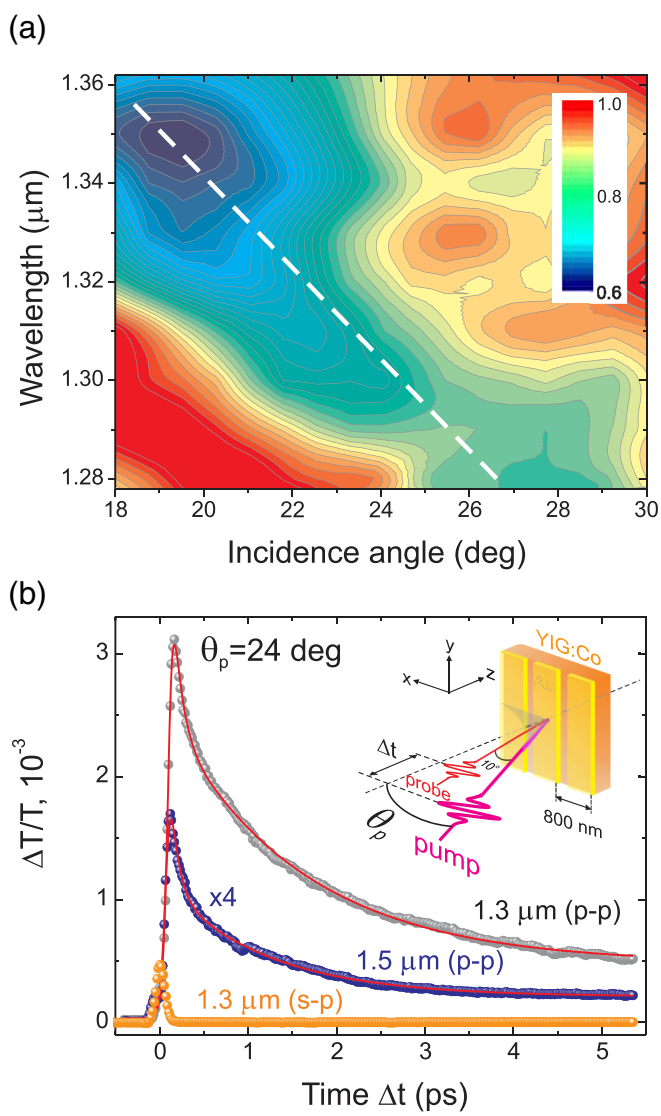

FIG. 2. (a) False color transmittivity map of the plasmonic Au-garnet grating. The low transmittivity area illustrates the SP dispersion, as highlighted with the white dashed line. The spectral width of the incident radiation is on the order of 50 nm. (b) Time-resolved transmittivity variations for the SP-resonant case (p-polarization, $\lambda_p = 1.3\ \mu$m) and two nonresonant cases. The red solid lines are the fit curves using Eq. (2). The inset: Schematics of the pump-probe experiments.

independently. The first term $\propto A_1$ describes spatial redistribution of the nonthermal electron population (transport) across the Au layer. Indeed, immediately after the laser excitation, hot carriers (electrons and holes) are created, modifying the optical properties of the metal due to the state-filling effect [33]. Owing to the spatial inhomogeneity of laser excitation, hot electron transport results in the in-depth equilibration of their distribution $n_N(z)$. In turn, the unequal in-depth sensitivity $s(z)$ of the probe beam to the state-filling effect results in transient variations of transmittance $\Delta T_N \propto \int_0^d n_N(z)s(z)dz$. This spatial redistribution proceeds with its own characteristic time τ_1 until the hot electron population is homogeneously distributed in Au. As such, τ_1 can be estimated as a mean electron travel time $\tau_1 \sim d/\langle v\rangle$, which in our case of ballistic transport yields $d/v_F \approx 50$ fs.

The second term in Eq. (1) ($\propto A_2$) describes local relaxation of nonthermal electron distribution n_N due to the electron scattering. Here we consider interactions of the ensemble of hot electrons with a combined reservoir consisting of electrons and phonons in the thermal equilibrium (Fig. 1, right). Eventually, both the electron and lattice temperatures increase, which is accounted for in the third term of Eq. (1) ($\propto A_3$). It results in an offset at large time delays since the heat dissipation away from the laser spot occurs at much longer timescales. This analytic function with two characteristic timescales τ_1, τ_2 provides excellent fits to the experimental transmittance traces [Fig. 2(b)].

IV. DISCUSSION

The data shown in Fig. 2(b) exemplify the difference between the electron response at and away from the SP resonance, in particular, the enhanced SP-induced variations ΔT. The blue data points were obtained at $\lambda_p = 1.5\ \mu$m, where no phase-matched SP excitation can be expected. From the fit procedure, we extract $\tau_1 \approx 58$ fs, $\tau_2 \approx 1.14$ ps, in a very good agreement with our expectations. We attribute τ_1 and τ_2 to the characteristic timescales of the electron transport and thermalization, respectively. In contrast, at the SP resonance $\lambda_p = 1.3\ \mu$m [Fig. 2(b), gray], we found $\tau_1 \approx 162$ fs, $\tau_2 \approx 1.52$ ps. Systematic measurements with λ_p varied around λ_{SP} allowed us to plot the resulting spectra of the amplitude of the variations $\Delta T/T(t)$ and τ_i in Fig. 3. The amplitude peaks at λ_{SP}, indicating the enhanced SP-induced photon absorption and hot electron generation [Fig. 3(a)]. Moreover, we found a consistent enhancement of τ_1 at the resonance, rising from $\approx$50 fs up to $\approx$200 fs [Fig. 3(b)]. A similar increase in the spectral dependence of τ_2 is concealed by the general nonresonant trend.

We note that the SP excitation cannot significantly modify the initial in-depth distribution of the hot electrons. Indeed, the SP electric field inside the metal exponentially decays away from the interface with the characteristic length $\xi \approx 22.7$ nm [54] at $\lambda = 1.3\ \mu$m ($\varepsilon_m \equiv \varepsilon_m' + i\varepsilon_m'' = -77.2 + 6.8i$ [55], $\varepsilon_d \approx 5$ [56]). This value is very close to the off-resonant penetration depth of the optical field $\zeta \approx 23.5$ nm. As such, the laser excitation profiles in Au in the resonant and nonresonant cases are very similar, and the enhanced electron transport timescale τ_1 cannot be explained by unequal initial population profiles of the primarily excited nonthermal hot electrons $n_N(z)$.

To explain this enhancement, we now briefly recall the conventional approach to the electron dynamics in metals. The two-temperature model [57] describes the interaction of the electron and phonon reservoirs in thermal equilibrium. In PMs, this picture is irrelevant on the sub-ps timescale, where nonthermal electrons are vital. The electron dynamics is usually obtained from rate equations, enabling the uncomplicated augmentation of the model with additional reservoirs such as nonthermal particles [10,23]. In the case of sufficiently inhomogeneous laser excitation, the electron transport can be taken into account in the form of superdiffusion. Importantly, on the ultrashort timescale, all other reservoirs can be omitted,

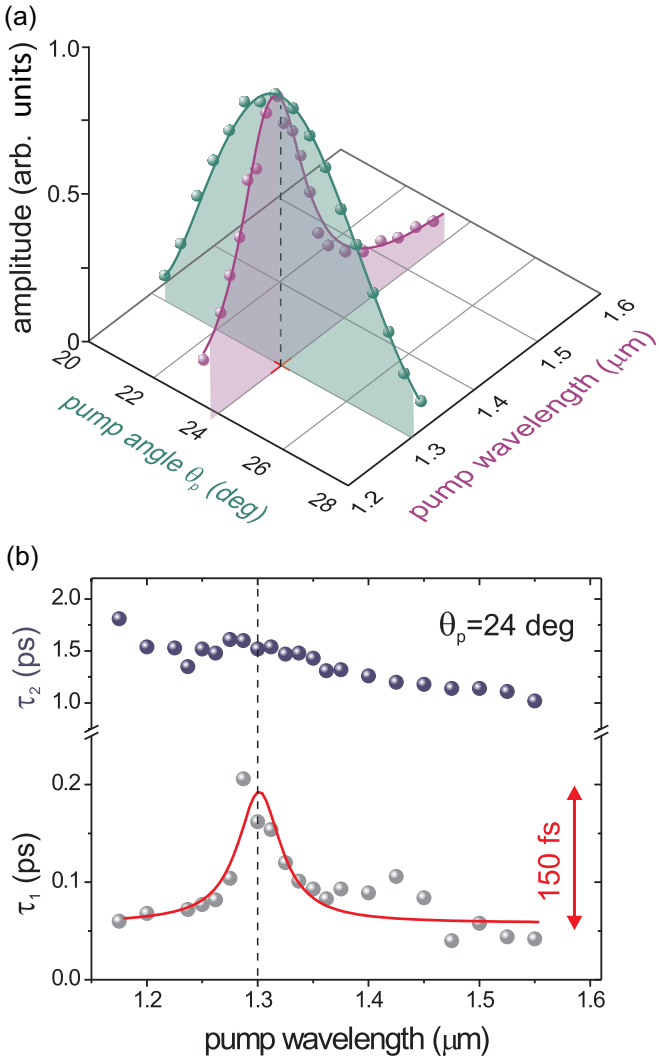

FIG. 3. (a) The amplitude of the pump-induced transmittance variations is strongly increased at $\lambda_p = 1.3$ μm, $\theta_p = 24^o$, corresponding to the SP excitation. The solid lines and shades are guides to the eye. (b) Spectral dependence of the hot electrons transport (τ_1, bottom) and thermalization (τ_2, top) timescales. The solid red line indicates the pronounced enhancement of τ_1 at the SP resonance ($\lambda_{SP} = 1.3$ μm).

and the dynamics of the hot nonthermal electrons $n_N(z,t)$ can be modeled as follows:

$$\frac{\partial n_N}{\partial t} = -\frac{n_N}{\tau_2} + D^\star \frac{\partial^2 n_N}{\partial z^2} + S(z,t), \tag{2}$$

where $D^\star$ is the generalized diffusion coefficient (in the diffusive limit $D^\star = \langle v \rangle l_e/3$), and $S(z,t)$ is the source term describing the excitation of hot electrons. This equation governs the dynamics of the nonthermal electrons on their own timescale τ_2. The SP lifetime on a *continuous* Au/garnet interface at 1.3 μm can be calculated [54,58] as $\tau_{SP} \approx 310$ fs. Because $\tau_{SP} \ll \tau_2$ [Fig. 3(b)], we can incorporate the SP excitation into Eq. (2) by modifying the source term S into a convolution of the laser excitation and the SP dynamics:

$$S_{SP}(z,t) = S(z,t) * Le^{-t/\tau_{SP}}. \tag{3}$$

Depending on the SP quality factor, the amplitude $L > 1$ illustrates SP-enhanced light absorption and hot electron generation in the metal. Here we neglect the spatial dependence of the SP-driven contribution $Le^{-t/\tau_{SP}}$ due to the aforementioned similarity of the light penetration profiles in the resonant and nonresonant cases. Thus the role of collective electronic excitations is revealed: SPs act as delayed sources of hot nonthermal electrons, extending the time period when the hot electron dynamics (both local and nonlocal) is relevant. The impact of the SP excitation with the lifetime $\tau_{SP} \sim 0.1$ ps is more noticeable in the nonlocal dynamics occurring on a similar timescale τ_1 than in the slower local electron thermalization ($\tau_2 \sim 1$ ps).

The similarity of the nonlocal relaxation of hot electrons and the SP decay timescales emphasizes the importance of spectrally resolved measurements where the transient optical response at the phase-matched SP resonance and away from it can be compared.

The periodicity of the Au/garnet grating enables radiative SP losses which add up to the intrinsic (joule) ones, reducing the SP lifetime τ'_{SP}. The data in Fig. 3(b) yields $\tau'_{SP} \approx 150$ fs, close to $\tau'_{SP} \sim \lambda^2/c\Delta\lambda \approx 120$ fs, where $\Delta\lambda \approx 50$ nm is the spectral width of the SP resonances. A pronounced SP resonance indicates the approximate balance of the joule and radiative losses [54], decreasing the SP lifetime on a grating by a factor of two, as compared to $\tau_{SP} \approx 310$ fs on a continuous interface, $\tau'_{SP} \approx \tau_{SP}/2$. An outstanding consistency in the determination of the SP lifetime strongly corroborates our understanding of the SP role in nonthermal electron dynamics.

To unambiguously associate the observed effects with the SP excitation, in the second run of experiments we fixed the pump wavelength at $\lambda_p = 1.3$ μm and varied the pump angle of incidence. We again fitted the function from Eq. (1) to the measured time-resolved transmittivity traces and extracted the fit parameters. Then, taking advantage of the interchangeability of λ_p and θ_p for the phase-matched SP excitation, we plotted the hot electron transport timescale τ_1 as a function of the in-plane momentum $k_{in} = k_0 \sin\theta_p$. We found a great degree of similarity between these sets of data obtained in the two independent measurements (Fig. 4). Remarkably, the only crossover of the two clearly distinct experimental approaches is the phase-matched SP excitation at $k_{in} = k_{SP} - mk_G$, thus unequivocally corroborating our understanding of the collective dynamics of nonthermal electrons. Within our framework, the data obtained in the two distinct series of measurements demonstrate increased hot electron lifetimes at the SP resonance and elucidate the role of SPs in hot electron dynamics.

V. CONCLUSIONS

Summarizing, we have performed time-resolved measurements of the hot electron dynamics in Au on the subpicosecond timescale in the vicinity of the SP resonance and shown how the time-resolved transmittivity data can be employed for the direct measurement of SP lifetimes at arbitrary corrugated interfaces with unknown losses. Systematic measurements with two independently varied parameters allowed us to unambiguously attribute the apparent retardation of the hot electron population decay to the SP excitation. Our results

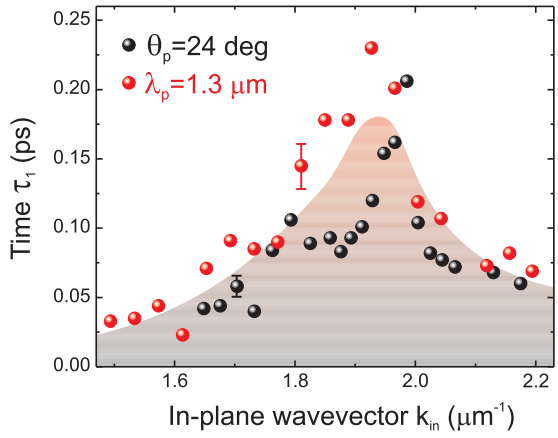

FIG. 4. The nonlocal relaxation time τ_1 as a function of the in-plane pump wave-vector component k_{in}, obtained from the experiments with varied λ_p (black, $\theta_p = 24^{\circ}$) and θ_p (red, $\lambda_p = 1.3\ \mu$m). The remarkable agreement of the two data sets confirms the SP resonance-driven τ_1 behavior illustrated with the shaded area.

clearly identify the role of SP resonances in the ultrafast optical response and significantly advance the understanding of collective hot electron dynamics. In particular, the engineering of nonthermal electron population can be key for the duration of the spin-polarized current pulses [26,59,60], spin Seebeck [61], and inverse spin-Hall [62] effects. Further applications entail spin-wave generation [46] and all-optical magnetization reversal [43,63], where SP-driven, nonlocal manipulation of nonthermal populations of electrons opens up additional possibilities for all-optical spin switching.

ACKNOWLEDGMENTS

The authors thank A. Melnikov and A. Kirilyuk for valuable comments and M. Wolf, T. V. Murzina, and A. Maziewski for their support. This work has been funded by the National Science Centre Poland (Grant No. DEC-2017/25/B/ST3/01305).

[1] S. Mukherjee, F. Libisch, N. Large, O. Neumann, L. V. Brown, J. Cheng, J. B. Lassiter, E. A. Carter, P. Nordlander, and N. J. Halas, Nano Lett. **13**, 240 (2013).
[2] C. Clavero, Nat. Photon. **8**, 95 (2014).
[3] A. Manjavacas, J. G. Liu, V. Kulkarni, and P. Nordlander, ACS Nano **8**, 7630 (2014).
[4] M. L. Brongersma, N. J. Halas, and P. Nordlander, Nat. Nanotech. **10**, 25 (2015).
[5] W. Li and J. G. Valentine, Nanophotonics **6**, 177 (2017).
[6] C. V. Hoang, K. Hayashi, Y. Ito, N. Gorai, G. Allison, X. Shi, Q. Sun, Z. Cheng, K. Ueno, K. Goda, and H. Misawa, Nat. Commun. **8**, 771 (2017).
[7] H. Shan, Y. Yu, X. Wang, Y. Luo, S. Zu, B. Du, T. Han, B. Li, Y. Li, J. Wu, F. Lin, K. Shi, B. K. Tay, Z. Liu, X. Zhu, and Z. Fang, Light: Sci. Appl. **8**, 9 (2019).
[8] W. S. Fann, R. Storz, H. W. K. Tom, and J. Bokor, Phys. Rev. B **46**, 13592 (1992).
[9] R. H. M. Groeneveld, R. Sprik, and A. Lagendijk, Phys. Rev. B **45**, 5079 (1992).
[10] C.-K. Sun, F. Vallée, L. H. Acioli, E. P. Ippen, and J. G. Fujimoto, Phys. Rev. B **50**, 15337 (1994).
[11] R. H. M. Groeneveld, R. Sprik, and A. Lagendijk, Phys. Rev. B **51**, 11433 (1995).
[12] N. Del Fatti, C. Voisin, M. Achermann, S. Tzortzakis, D. Christofilos, and F. Vallée, Phys. Rev. B **61**, 16956 (2000).
[13] B. Rethfeld, A. Kaiser, M. Vicanek, and G. Simon, Phys. Rev. B **65**, 214303 (2002).
[14] B. Y. Mueller and B. Rethfeld, Phys. Rev. B **87**, 035139 (2013).
[15] R. Sundararaman, P. Narang, A. S. Jermyn, W. A. Goddard, III, and H. A. Atwater, Nat. Commun. **5**, 5788 (2014).
[16] G. Chen, Phys. Rev. Lett. **86**, 2297 (2001).
[17] J.-Y. Bigot, J.-Y. Merle, O. Cregut, and A. Daunois, Phys. Rev. Lett. **75**, 4702 (1995).
[18] B. Lamprecht, G. Schider, R. T. Lechner, H. Ditlbacher, J. R. Krenn, A. Leitner, and F. R. Aussenegg, Phys. Rev. Lett. **84**, 4721 (2000).
[19] J. Lehmann, M. Merschdorf, W. Pfeiffer, A. Thon, S. Voll, and G. Gerber, Phys. Rev. Lett. **85**, 2921 (2000).
[20] C. Voisin, N. Del Fatti, D. Christofilos, and F. Vallée, J. Phys. Chem. B **105**, 2264 (2001).
[21] J. R. M. Saavedra, A. Asenjo-Garcia, and F. J. Garcia de Abajo, ACS Photonics **3**, 1637 (2016).
[22] A. M. Brown, R. Sundararaman, P. Narang, A. M. Schwartzberg, W. A. Goddard, and H. A. Atwater, Phys. Rev. Lett. **118**, 087401 (2017).
[23] N. Rotenberg, J. N. Caspers, and H. M. van Driel, Phys. Rev. B **80**, 245420 (2009).
[24] M. Lejman, V. Shalagatskyi, O. Kovalenko, T. Pezeril, V. V. Temnov, and P. Ruello, J. Opt. Soc. Am. B **31**, 282 (2014).
[25] A. Melnikov, I. Razdolski, T. O. Wehling, E. T. Papaioannou, V. Roddatis, P. Fumagalli, O. Aktsipetrov, A. I. Lichtenstein, and U. Bovensiepen, Phys. Rev. Lett. **107**, 076601 (2011).
[26] A. Alekhin, I. Razdolski, N. Ilin, J. P. Meyburg, D. Diesing, V. Roddatis, I. Rungger, M. Stamenova, S. Sanvito, U. Bovensiepen, and A. Melnikov, Phys. Rev. Lett. **119**, 017202 (2017).
[27] G. Malinowski, F. Dalla Longa, J. H. H. Rietjens, P. V. Paluskar, R. Huijink, H. J. M. Swagten, and B. Koopmans, Nat. Phys. **4**, 855 (2008).
[28] M. Battiato, K. Carva, and P. M. Oppeneer, Phys. Rev. Lett. **105**, 027203 (2010).
[29] A. Eschenlohr, M. Battiato, P. Maldonado, N. Pontius, T. Kachel, K. Holldack, R. Mitzner, A. Föhlisch, P. M. Oppeneer, and C. Stamm, Nat. Mater. **12**, 332 (2013).
[30] A. J. Schellekens, W. Verhoeven, T. N. Vader, and B. Koopmans, Appl. Phys. Lett. **102**, 252408 (2013).
[31] J. Wieczorek, A. Eschenlohr, B. Weidtmann, M. Rösner, N. Bergeard, A. Tarasevitch, T. O. Wehling, and U. Bovensiepen, Phys. Rev. B **92**, 174410 (2015).
[32] N. Bergeard, M. Hehn, S. Mangin, G. Lengaigne, F. Montaigne, M. L. M. Lalieu, B. Koopmans, and G. Malinowski, Phys. Rev. Lett. **117**, 147203 (2016).

[33] I. Razdolski, A. Alekhin, U. Martens, D. Bürstel, D. Diesing, M. Münzenberg, U. Bovensiepen, and A. Melnikov, J. Phys.: Condens. Matter **29**, 174002 (2017).
[34] S. D. Brorson, J. G. Fujimoto, and E. P. Ippen, Phys. Rev. Lett. **59**, 1962 (1987).
[35] M. Battiato, K. Carva, and P. M. Oppeneer, Phys. Rev. B **86**, 024404 (2012).
[36] W. F. Krolikowski and W. E. Spicer, Phys. Rev. B **1**, 478 (1970).
[37] T. Juhasz, H. E. Elsayed-Ali, G. O. Smith, C. Suárez, and W. E. Bron, Phys. Rev. B **48**, 15488 (1993).
[38] J. Hohlfeld, J. Müller, S.-S. Wellershoff, and E. Matthias, Appl. Phys. B **64**, 387 (1997).
[39] C. A. Schmuttenmaer, M. Aeschlimann, H. E. Elsayed-Ali, R. J. D. Miller, D. A. Mantell, J. Cao, and Y. Gao, Phys. Rev. B **50**, 8957 (1994).
[40] E. Knoesel, A. Hotzel, T. Hertel, M. Wolf, and G. Ertl, Surf. Sci. **368**, 76 (1996).
[41] M. Bauer, A. Marienfeld, and M. Aeschlimann, Prog. Surf. Sci. **90**, 319 (2015).
[42] F. Spitzer, B. A. Glavin, V. I. Belotelov, J. Vondran, I. A. Akimov, S. Kasture, V. G. Achanta, D. R. Yakovlev, and M. Bayer, Phys. Rev. B **94**, 201118(R) (2016).
[43] A. Stupakiewicz, K. Szerenos, D. Afanasiev, A. Kirilyuk, and A. V. Kimel, Nature **542**, 71 (2017).
[44] C. von Korff Schmising, M. Giovannella, D. Weder, S. Schaffert, J. L. Webb, and S. Eisebitt, New J. Phys. **17**, 033047 (2015).
[45] T.-M. Liu, T. Wang, A. H. Reid, M. Savoini, X. Wu, B. Koene, P. Granitzka, C. E. Graves, D. J. Higley, Z. Chen, G. Razinskas, M. Hantschmann, A. Scherz, J. Stöhr, A. Tsukamoto, B. Hecht, A. V. Kimel, A. Kirilyuk, T. Rasing, and H. A. Dürr, Nano Lett. **15**, 6862 (2015).
[46] A. L. Chekhov, A. I. Stognij, T. Satoh, T. V. Murzina, I. Razdolski, and A. Stupakiewicz, Nano Lett. **18**, 2970 (2018).
[47] V. I. Belotelov, I. A. Akimov, M. Pohl, V. A. Kotov, S. Kasture, A. S. Vengurlekar, A. V. Gopal, D. R. Yakovlev, A. K. Zvezdin, and M. Bayer, Nat. Nanotech. **6**, 370 (2011).
[48] V. I. Belotelov, L. E. Kreilkamp, I. A. Akimov, A. N. Kalish, D. A. Bykov, S. Kasture, V. J. Yallapragada, A. Venu Gopal, A. M. Grishin, S. I. Khartsev, M. Nur-E-Alam, M. Vasiliev, L. L. Doskolovich, D. R. Yakovlev, K. Alameh, A. K. Zvezdin, and M. Bayer, Nat. Commun. **4**, 2128 (2013).
[49] J. Y. Chin, T. Steinle, T. Wehlus, D. Dregely, T. Weiss, V. I. Belotelov, B. Stritzker, and H. Giessen, Nat. Commun. **4**, 1599 (2013).
[50] M. Pohl, V. I. Belotelov, I. A. Akimov, S. Kasture, A. S. Vengurlekar, A. V. Gopal, A. K. Zvezdin, D. R. Yakovlev, and M. Bayer, Phys. Rev. B **85**, 081401(R) (2012).
[51] V. L. Krutyanskiy, A. L. Chekhov, V. A. Ketsko, A. I. Stognij, and T. V. Murzina, Phys. Rev. B **91**, 121411(R) (2015).
[52] I. Razdolski, S. Parchenko, A. Stupakiewicz, S. Semin, A. Stognij, A. Maziewski, A. Kirilyuk, and T. Rasing, ACS Photonics **2**, 20 (2015).
[53] A. L. Chekhov, I. Razdolski, A. Kirilyuk, T. Rasing, A. I. Stognij, and T. V. Murzina, Phys. Rev. B **93**, 161405(R) (2016).
[54] H. Raether, *Surface Plasmons on Smooth and Rough Surfaces and on Gratings*, Springer Tracts in Modern Physics, Vol. 111 (Springer-Verlag, Berlin, 1988).
[55] P. B. Johnson and R. W. Christy, Phys. Rev. B **6**, 4370 (1972).
[56] Magnetic properties of non-metallic inorganic compounds based on transition elements, in *Landolt-Börstein, Numerical Data and Functional Relationships in Science and Technology*, Vol. 27E, edited by H. Wijn (Springer-Verlag, Berlin, 1991).
[57] S. Anisimov, B. Kapeliovich, and T. Perelman, Zh. Exp. Teor. Fiz. **66**, 776 (1974).
[58] T. J.-Y. Derrien, J. Krüger, and J. Bonse, J. Opt. **18**, 115007 (2016).
[59] I. Razdolski, A. Alekhin, N. Ilin, J. P. Meyburg, V. Roddatis, D. Diesing, U. Bovensiepen, and A. Melnikov, Nat. Commun. **8**, 15007 (2017).
[60] M. L. M. Lalieu, P. L. J. Helgers, and B. Koopmans, Phys. Rev. B **96**, 014417 (2017).
[61] J. Kimling, G.-M. Choi, J. T. Brangham, T. Matalla-Wagner, T. Huebner, T. Kuschel, F. Yang, and D. G. Cahill, Phys. Rev. Lett. **118**, 057201 (2017).
[62] T. S. Seifert, S. Jaiswal, J. Barker, S. T. Weber, I. Razdolski, J. Cramer, O. Gueckstock, S. F. Maehrlein, L. Nadvornik, S. Watanabe, C. Ciccarelli, A. Melnikov, G. Jakob, M. Münzenberg, S. T. B. Goennenwein, G. Woltersdorf, B. Rethfeld, P. W. Brouwer, M. Wolf, M. Kläui, and T. Kampfrath, Nat. Commun. **9**, 2899 (2018).
[63] A. Stupakiewicz, K. Szerenos, M. D. Davydova, K. A. Zvezdin, A. K. Zvezdin, A. Kirilyuk, and A. V. Kimel, Nat. Commun. **10**, 612 (2019).